Supplement file for "Striatal Subdivisions Estimated via Deep Embedded Clustering with Application to Parkinson's Disease"

Yu Li, Aiping Liu*, Taomian Mi, Runyu Yang, Piu Chan, Martin J. McKeown, Xun Chen, *Senior Member, IEEE* and Feng Wu, *Fellow, IEEE*

In this supplemental file, to explore the effects of nonlinear features extracted by our framework, we compared the reproducibility and functional homogeneity of our results and those of three clustering methods combined with linear a dimensional reduction algorithm (i.e., PCA) (see Fig. S2, Fig. S3, and Fig. S5). In Fig. S4, we also estimated and compared the intra-subject reproducibility on the NYU dataset based on the trained Beijing model. Fig. S1 is the results of sensitivity analysis on 3-parcel parcellation. For all parcel numbers, we provided the overlap rate between the regions showing positive sensitivity analysis value and the subregions (TABLE SI), and the percentage of these overlapped regions to the subregions (TABLE SII). Furthermore, we provided the results of ROI-to-ROI analyses based on 6-parcel parcellation and based on Brainnetome atlas; see TABLE SIII, SIV, and Fig. S6.

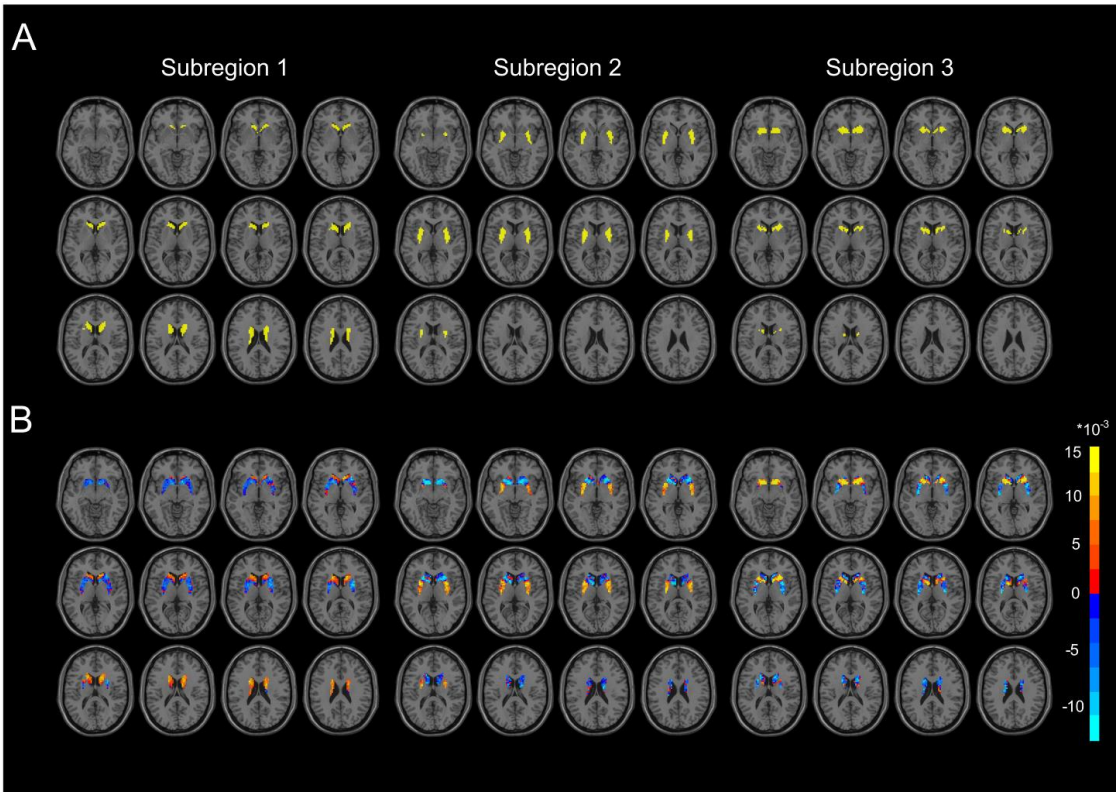

Fig. S1. (A) The striatal parcellations of DECBP with parcel number 3. (B) Sensitivity analysis for each subregion. Sensitivity analysis calculates the partial derivatives of DECBP output (the probability of input voxel belonging to each subregion) with respect to input features (the similarity of FC between input voxel and striatal voxels). For each voxel of each subregion (column), the positive value indicate that the more similar FC pattern between the unassigned voxel and this voxel is, the more possibly that unassigned voxel belong to this subregion.

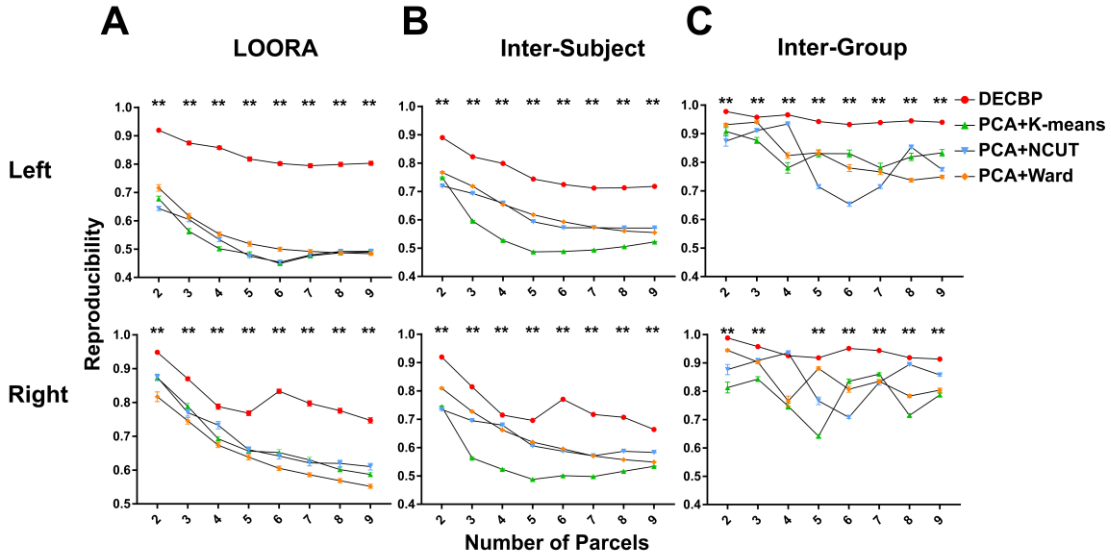

Fig. S2. Comparisons of reproducibility on inter-individual and group level. (A) Inter-individual reproducibility based on LOORA method. (B) Inter-individual reproducibility measured using all pairs of subjects. (C) Group reproducibility. The asterisk denotes that the reproducibility of DECBP significantly higher than other methods (*$p < 0.05$; **, $p < 0.001$). Top and bottom rows denote the results of left and right striatum, respectively. LOORA, leave-one-out reproducibility analysis; DECBP, deep embedded connectivity-based parcellation; PCA, principal components analysis; PCA+K-means, K-means clustering combined with PCA; PCA+NCUT, normalized-cut spectral clustering combined with PCA; PCA+Ward, Ward's hierarchical clustering combined with PCA.

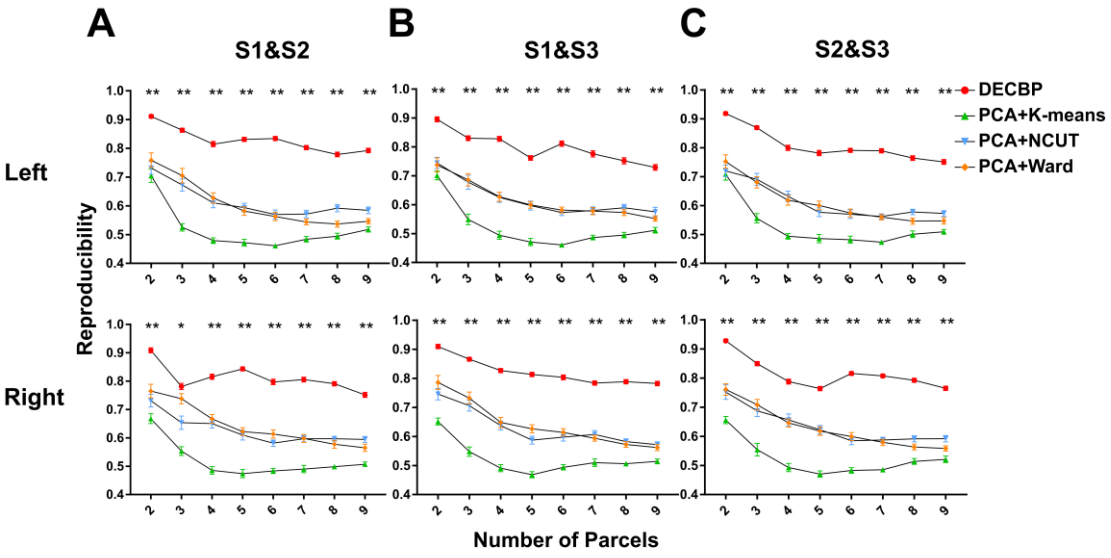

Fig. S3. Comparisons of reproducibility between any two of the three scans. The asterisk denotes that the reproducibility of DECBP significantly higher than other methods (*, $p < 0.05$; **, $p < 0.001$). Top and bottom rows denote the results of left and right striatum, respectively. S1, Scan 1; S2, Scan 2; S3, Scan 3; DECBP, deep embedded connectivity-based parcellation; PCA, principal components analysis; PCA+K-means, K-means clustering combined with PCA; PCA+NCUT, normalized-cut spectral clustering combined with PCA; PCA+Ward, Ward's hierarchical clustering combined with PCA.

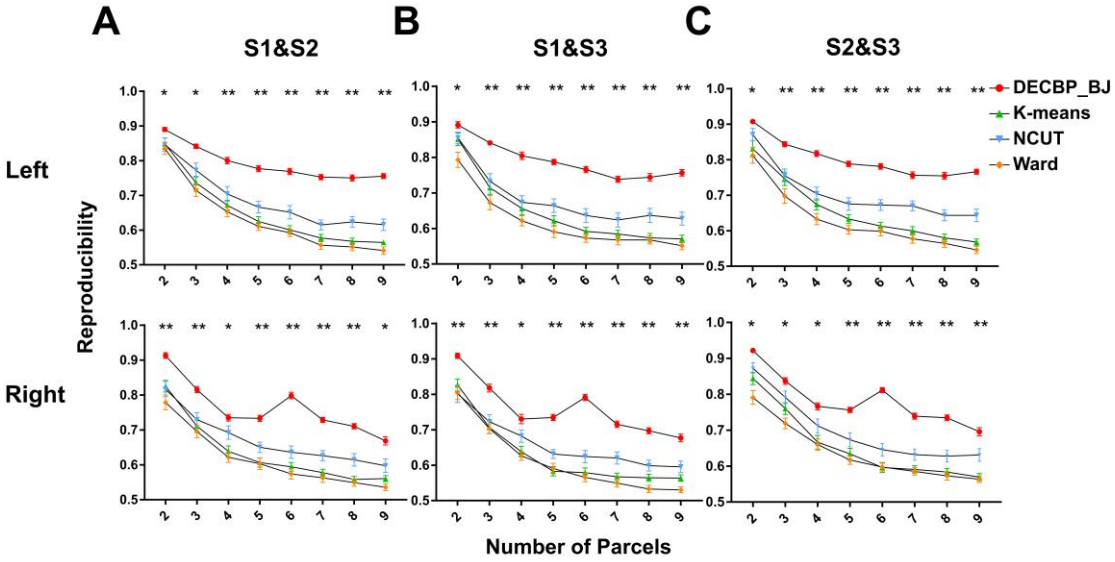

Fig. S4. Comparisons of reproducibility between any two of the three scans. The asterisk denotes that the reproducibility of DECBP significantly higher than other methods (*, $p < 0.05$; **, $p < 0.001$). Top and bottom rows denote the results of left and right striatum, respectively. S1, Scan 1; S2, Scan 2; S3, Scan 3; DECBP_BJ, deep embedded connectivity-based parcellation using the trained Beijing model; Ward, Ward's hierarchical clustering method; NCUT, normalized-cut spectral clustering method.

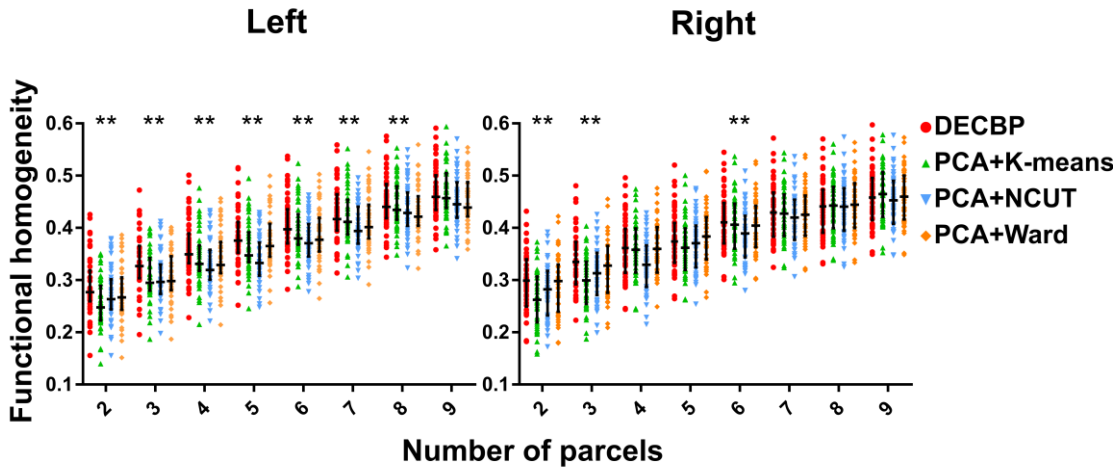

Fig. S5. Comparisons of functional homogeneity in left and right striatum. For each error bar, the central mark is the median, and edges are the 25th and 75th percentiles. The asterisk denotes that DECBP significantly better than other methods (**, $p < 0.001$). DECBP, deep embedded connectivity-based parcellation; PCA, principal components analysis; PCA+K-means, K-means clustering combined with PCA; PCA+NCUT, normalized-cut spectral clustering combined with PCA; PCA+Ward, Ward's hierarchical clustering combined with PCA.

TABLE SI
MEAN OVERLAP (DICE) BETWEEN THE REGION SHOWING POSITIVE VALUE IN SENSITIVITY ANALYSIS AND THE SUBREGION

The Number of Parcels	Left Striatum	Right Striatum	Mean
2	0.937	0.916	0.9265
3	0.844	0.850	0.847
4	0.742	0.728	0.735
5	0.615	0.581	0.598
6	0.537	0.574	0.5555
7	0.482	0.497	0.4895
8	0.440	0.449	0.4445
9	0.398	0.409	0.4035

TABLE SII
PERCENTAGE OF THE NUMBER OF SUBREGIONAL VOXELS SHOWING POSITIVE VALUE IN SENSITIVITY ANALYSIS TO THE NUMBER OF SUBREGIONAL VOXELS

The Number of Parcels	Left Striatum	Right Striatum	Mean
2	0.936	0.916	0.926
3	0.960	0.949	0.9545
4	0.984	0.951	0.9675
5	0.983	0.940	0.9615
6	0.986	0.981	0.9835
7	0.994	0.991	0.9925
8	0.990	0.985	0.9875
9	0.984	0.992	0.988

TABLE SIII
COMPARISON OF ROI-TO-ROI CONNECTIVITY BETWEEN THE PD AND HC GROUPS BASED ON 6-PARCEL PARCELLATION

Connections	*p* value	*T* value
Regions connected with left rostral putamen		
Cerebelum_7b_L	5.06×10^{-5}	-4.48
Regions connected with left ventral putamen		
IFGoper_R	3.28×10^{-4}	-3.89
Pallidum_R	1.14×10^{-6}	-5.62
Regions connected with left caudal putamen		
Precentral gyrus_L	2.77×10^{-5}	-4.67
Precentral gyrus_R	1.15×10^{-4}	-4.22
IFGoper_L	2.17×10^{-4}	-4.02
IFGoper_R	5.17×10^{-5}	-4.47
Rolandic operculum_R	3.02×10^{-4}	-3.92
Supplementary motor area_L	3.33×10^{-5}	-4.61
Supplementary motor area_R	1.11×10^{-4}	-4.24
Median cingulate gyrus_L	1.97×10^{-4}	-4.05
Median cingulate gyrus_R	1.17×10^{-4}	-4.22
Inferior parietal lobule_L	2.40×10^{-4}	-3.99
Inferior parietal lobule_R	2.28×10^{-4}	-4.01
Pallidum_L	3.82×10^{-5}	-4.57
Pallidum_R	1.25×10^{-6}	-5.59
Regions connected with right rostral caudate		
Heschl gyrus_R	4.29×10^{-4}	3.80
Regions connected with right rostral putamen		
Angular gyrus_L	1.44×10^{-4}	-4.15
Cerebelum_Crus2_L	1.96×10^{-4}	-4.06
Cerebelum_7b_L	1.51×10^{-4}	-4.14
Regions connected with right ventral putamen		
Middle frontal gyrus_L	9.28×10^{-5}	-4.29
IFGtri_L	2.84×10^{-4}	-3.94
Pallidum_L	2.01×10^{-4}	-4.05
Regions connected with right caudal putamen		
Pallidum_L	1.08×10^{-4}	-4.25

IFGoper, Inferior frontal gyrus, opercular part; IFGtri, Inferior frontal gyrus, triangular part; L, left; R, right. $T < 0$, PD < HC.

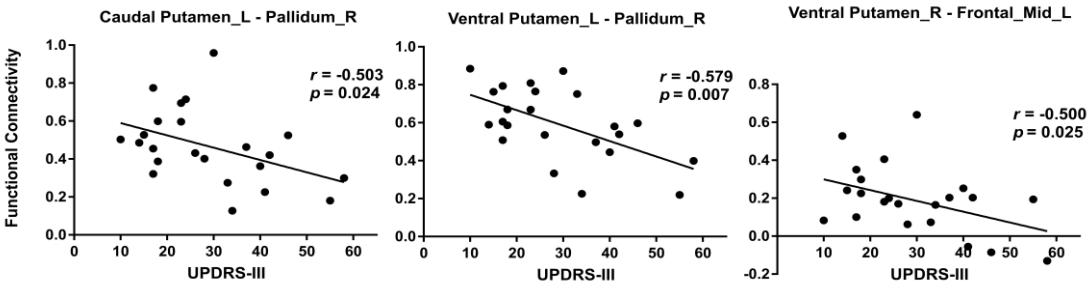

Fig. S6. Correlation of functional connectivity with PD severity based on 6-parcel parcellation of striatum.

TABLE SIV
BETWEEN-GROUP DIFFERENCE OF CONNECTIVITY BETWEEN 3-PARCEL STRIATAL SUBDIVISIONS AND OTHER BRAIN REGIONS OF BRAINNETOME ATLAS

Connections	*p* value	*T* value
Regions connected with left Caudate		

dIg, dorsal granular insula	1.26×10^{-4}	4.20
Regions connected with left Ant putamen		
MFG, inferior frontal junction _L	1.42×10^{-4}	-4.16
MFG, inferior frontal junction _R	2.05×10^{-4}	-4.04
IFG, opercular area 44 _L	6.67×10^{-5}	-4.40
Regions connected with left Pos putamen		
IFG, dorsal area 44_R	7.09×10^{-5}	-4.38
IFG, opercular area 44 _L	5.32×10^{-5}	-4.47
IFG, opercular area 44_R	9.76×10^{-5}	-4.28
IFG, ventral area 44_R	1.47×10^{-4}	-4.15
Precentral Gyrus, caudal ventrolateral area 6 _L	3.49×10^{-5}	-4.60
Precentral Gyrus, caudal ventrolateral area 6 _R	1.51×10^{-5}	-4.85
globus pallidus_R	7.92×10^{-5}	-4.34
Regions connected with right Ant putamen		
MFG, dorsal area 9/46_L	8.15×10^{-5}	-4.33

Ant, anterior; Pos, posterior; IFG, Inferior frontal gyrus; MFG, Middle Frontal Gyrus; L, left; R, right. $T < 0$, PD < HC.